Preparation and Characterization of Zn0.9 Sc0.1O, Zn0.9 Mn0.1OParticles and Comparison with the Pristine ZnO-NPs by Using Co- precipitation Method

Mariam ghassan   **Shaker J. Edrees**

Department of Ceramics and Building Materials, Collage of Materials Engineering, University of Babylon

Corresponding author. E-mail address: mariam35ghassan@gmail.com

Abstract

This is a pure and Scandium (Sc+3), Manganese (Mn+3) were added to ZnO in different controlled percentages Zn(1-x) ScxO, Zn(1-x) MnxO. Synthesized using a co-precipitation technique. Particularly, it was demonstrated that several novel and intriguing physical properties. These were created by means of a combination of morphological-structural and optical research. X-ray diffraction research explained that the ZnO hexagonal wurtzite structure was preserved alongside the (002) preferred crystallized plane for ZnO with (Sc,Mn)ions added .The particles were examined using field emission scanning electron microscopy shows the hemispherical shape and shows the increase in amount of manganese, as well the higher agglomeration. A distinct magnetization was indicated by the vibrating sample magnetometer test, which was utilized to obtain the hysteresis loops. ZnO-NPs showing at room temperature ferromagnetic (RTFM) characteristic.

Keywords, Diluted Magnetic Semiconductors, ZnO, Manganese, Scandium, XRD, FESEM, VSM

Introduction

Dilute magnetic semiconductors (DMS) that made of zinc oxide (ZnO) were gained a lot of research attention [1]. This is due to they offer a lot of potential for use in the various room-temperature electromagnetic devices [2]. As a result of its broad band gap (˜ 3.4 eV), high exciting binding energy at ambient temperature(˜60 meV), short luminescence lifetime, and other factors [3],excellent mechanical and chemical stability [4]. Because of the general lack of stoichiometry, primarily caused by oxygen vacancies, ZnO is often an n-type wide-gap semiconductor [5].These vacancies cause the band gap to generate deep trap levels [6]. ZnO may have its physicochemical properties, for instance, its crystallographic , morphological, optical, electrical, and the magnetic properties, controlled by doping it with M(+3) elements (M=In, Ga, Sc, Y, Mn , Al, B, and Tl) [7]. How effective doping substances is functions was determined by the difference in ionic radius between the doping and host atoms [8]. It is a viable contender due to these characteristics for the fabrication of the several optoelectronic, sensor, photo-catalyst, and magneto-optical devices. Nowadays studies are

bingeing conducted on the optical characteristics of nanostructured ZnO that has been doped with transition metals. This is due in response to the high demand for nanostructured optoelectronic devices in the future [9]. Many methods were developed to create a (Sc,Mn) doped ZnO nanoparticles. The research decided the co-precipitation method because it is a controlled wet chemical method that allows for easier sample fabrication with greater homogeneity. The study also studied the structural and optical properties of the (Sc,Mn) doped ZnO nanoparticles[10].

Materials and Methods

The precursor materials were directly employed in the formation of nanocrystallites. The pure form of ZnO was synthesized by co-precipitation in this work as follows first sample: 6.11g of zinc nitrate hexahydrate in 50 ml of water that was constantly stirred, zinc nitrate hexahydrate is made. Then, 4.312g of citric acid that was dissolved in 50ml of water and slowly added to the above solution with the stirring constantly at 70-80°C for 2 hours.

In the same time second sample, for dopant, a mixture of zinc nitrate hexahydrate (Zn (NO3)2. 6H2O), Scandium nitrate (Sc (NO3)3) and third sample mixture of zinc nitrate hexahydrate (Zn (NO3)2. 6H2O), Manganese nitrate (Mn(NO3)3) was stirred in DI water until the concentrations of both are equal. Three samples were prepared pure ZnO , Zn(1-x) ScxO and sample was prepared from Zn(1-x) Mnx O with (x=10 wt%) to study the effect of the manganese, Scandium ion individually. Then, 50 ml of citric acid was slowly added to the above solution, then mixed for 2 hours at 70-80°C. The gel formed from both processes was dehydrated in an oven at 120°C for 3 hours. The Nano crystallites were crushed with a mortar and pestle before being annealed at 400°C for further characterization. The Starting materials in Co-Precipitation method shown in table1

Table1: The Starting materials in Co-Precipitation method.

Material name	Chemical Formula	Purity	Physical state
Zinc nitrate hydrate	$Zn(NO_3)_2.6 H_2O$	99.99	Solid
Scandium nitrate	$Sc(NO_3)_3$	99.99	Solid
		99.99	Solid
Manganese nitrate	$Mn(NO_3)_3$	99.99	Solid
Citric acid	$C_6H_8O_7$	----	Liquid
distilled water	H_2O		

1. Results and Discussion

3.1 Structural Properties

The XRD patterns of the main phase and $Zn_{(1-x)}Sc_x O$, $Zn_{(1-x)}Mn_x O$ where (x=10%wt) doped ZnO Nanostructures are shown in (Figure1 a) after the being calcinated at 400C° for 45 minutes . Each and every diffraction peak were identified as pure the hexagonal-wuartzite structure of ZnO. The identified peaks was consistent with the standard diffraction reflections for (ICDD 01-074-0534) , the space group P63mc the lattice parameters a = 3.245 A ° and c = 5.207 A °. There is no traces of other impurities like $Zn(OH)_2$, Sc_2O_3, Mn_2O_3 , it was observed that the amount of scandium and manganese is less than the limits for solubility. But the study doesn't exclude the possibility that clusters or precipitates of the secondary amorphous phase will form and be small enough that the XRD readings won't show.

The intensity of the XRD lines increased as the doping with Scandium and intensity of the XRD lines decreased as the doping with manganese, the FWHM expanded relative to the pure ZnO-NRs and the XRD lines' intensity fell (Sc,Mn 0.1%). This could mean that, in the comparison to the un-doped ZnO-NPs, the doped specimens displayed lower coherent domain sizes and increased crystallinity. Sc-doped ZnO's diffraction peak (2θ = 34.262°) was moved across lower angles compared to the pristine ZnO-NPs (2θ =34.409 °), Mn-doped ZnO's diffraction peak (2θ = 34.358°) was moved across higher angles after the angle was less in scandium compared to the pristine ZnO-NPs as shown in (Figure 1 b). The results were consistent with prior reports [11-12]. All patterns are in the single-phase, with no diffraction peaks from related oxide. This is because Sc^{3+} has an ionic radius (0.75 A°) that is slightly greater than Zn(0.74A°) ,Mn^{+3} has a slightly smaller ionic radius (0.66 A°) than Zn (0.74 A°). This pattern aligns with the earlier experimental reports. [11-13].

Peak shifting maybe a sign that strain formed in the ZnO lattice host and that the Zn^{+2}ions' crystallographic sites were successfully occupied by Sc^{+3} , Mn^{+3}ions. Moreover, by increasing the concentration of the manganese ion to ZnO, the diffraction peaks shifted towards a higher wavelength . The results are in line with earlier Manuscripts [11-13]. As the doping Sc, XRD lines' intensity increased, Mn XRD lines' intensity decreased, XRD peaks broadening (FWHM) were decrease, this is relative to the pure ZnO-NRs and the XRD lines' was more intense. This could explain in the comparison to the un-doped ZnO-NPs, the doped specimens displayed lower coherent domain sizes and increased crystallinity. All patterns are the single-phase, with no diffraction peaks from related oxide.This pattern aligns with the earlier experimental manuscripts [11-13].

The Scherrer equation was used to determine of the average crystallite size, through using the full width at half maximum (FWHM) of the diffraction peaks, for (100), (002), and (101) planes are the strongest in order to get the average coherent domain size according to the equation [14].

$$D = k \lambda / \beta \cos \theta \quad \ldots\ldots..(1)$$

The geometrical constant is k (0.9), D is the domain size, and λ is the wavelength of the used X-ray (λ = 1.5406 A). Where the diffraction angle is the diffraction peak's FWHM, and the

geometrical variable. The average grain sizes scandium, manganese doped zinc were found to be in the (10.31, 10.70 nm) which indicates that the samples are Nano crystalline. For the pristine ZnO-NPs, the obtained crystallite size was 18.24 nm. This result is in the complete agreement with the previous experimental calculations. The crystallite size of the doped samples were decrease slightly in (0.1 Sc^{+3}) then increased in (0.1 Mn^{+3}) as compared to the pure state. The lattice parameter for pure ZnO NPs is shown in Table2. The pure ZnO NPs is equal to (3.249, 5.205 Å), whereas for doped samples were raised. The lattice parameter can increase to a maximum of (3.264, 5.219Å) at (x=0.1) .The strongest diffraction peak's intensity (2θ=36.2766) along the (101) plane was decrease.

\

Table (2) Structure Factors of Doped and un-doped ZnO

Sample	crystallite size (nm) along (100) (002) and	Space Group	Lattice parameter (°A)	d-spacing (°A)
Pure	18.24	186#	8.4542	2.475 23
Sc%10	10.31	186#	8.4842	2.486 06
Mn%10	10.70	186#	8.4564	2.475 70
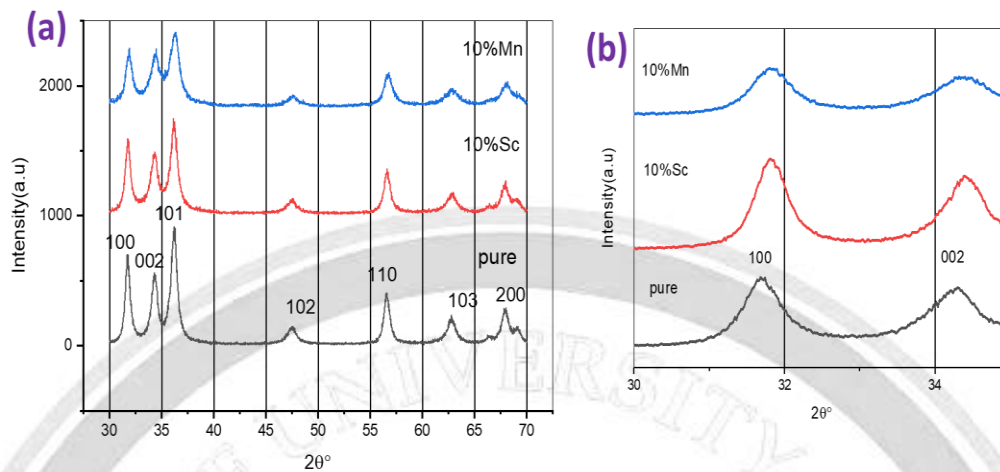
Figure 1. (a) XRD Pattern of Doped and Un-doped ZnO

(b) Shifting of Doped and Un-doped ZnO for (100) and (002) plan

3.2 FESEM Observations

Figures 2 shows the typical FESEM images respectively, of ZnO pure and ZnO/Sc , ZnO/ Mn (10 wt. %) annealed at the optimum temperature of 400 °C in air atmosphere for 1 h. FESEM is mainly used to analyzing the surface topography of the sample.The particles show semispherical shape, and these particles are in the highly agglomerated form (Figure2 a) demonstrates the pure ZnO nanoparticles as seen in FESEM pictures. It shows that the ZnO nanoparticles as seen in FESEM pictures. It shows that the ZnO nano-crystallites are uniformly sized and spherical in shape .Larger-sized ZnO is produced through the agglomeration of ZnO nanoparticles. Very little interparticle pore development occurs. The annealing temperature and the molar concentration of the precursor utilized for synthesis may be to blame for this. (Figure 2 b) it presents SEM photos of the powder samples doped with Sc^{+3} it shows that no discernible change in the particle morphology. Nearly all of the samples have aggregates of heterogeneous spherical nanoparticles as their primary morphology. However, particle size tends to decrease and change the surface shape as Sc^{+3} doping increase. The higher agglomeration is seen as the manganese concentration rises. SEM images of ZnO and ZnO doped with 10wt%Mn samples are shown in (Fig2 a and c), respectively. Un even globular particles were produced by pure ZnO SEM image of 10wt%Mn sample.
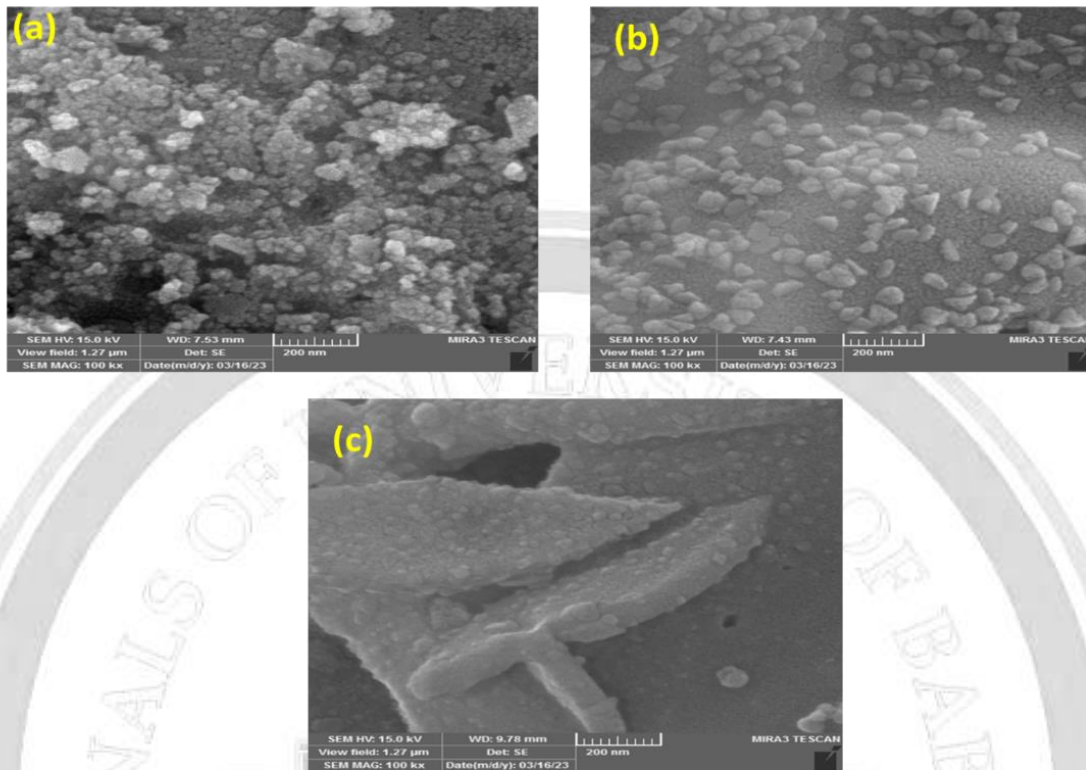
Figure2. FE-SEM Images (a) Pure ZnO Nanostructures and (b) ZnO/Sc- 10wt%

(c)ZnO/Mn-10wt%

At SEM micrographs the purity of the ZnO oxide was visible in the EDS micrograph. Zn and O were the only elements present in the sample. Zn and O were discovered to have weight percentages and atomicity of 73.15, 40.01, and 26.85, 59.99, respectively, which are similar to the weight % of bulk ZnO (80 for Zn and 20 for O). Zn and O were found to have weight percentages and atomicity of 77.47, 22.53, and 54.3, 45.7, respectively. According to EDS report the weight percentage and atomicity of Zn, Sc^{+3} and O were discovered to have weight percentages and atomicity of 76.98, 19.14, 3.88, and 47.86, 48.63, 3.50, respectively. The spectra revealed Zn signals at approximately 1 keV and 8.6 keV, as well as the oxygen peak at about 0.52 keV. Furthermore, at about 4.3 keV [12]. The peaks corresponding to Sc^{+3} have been seen. The kind and percentage by weight of each component in the chosen sample point are provided by the EDX. The study can distinguish between the EDX analyses of un-doped and doped ZnO, which led to a rise in the percentage of Sc^{+3} ions and a decrease in Zn^{+2} ions. Moreover, EDX examination showed that the highest proportion of zinc atoms is 76.98% at the ratio of scandium ions (10wt %), which strongly shows that the introduction of Sc^{+3} came at the expense of Zn^{+2}. The findings of the EDX study reveal that the amount of Zn^{+2} and Sc^{+3} ions when comparing the final powder to their load, they are not only similar but also quite compatible with one another. The kind and weight % of each element present in the chosen point of the samples are

provided by the EDX. The study can distinguish between un-doped and doped ZnO based on their EDX analyses. This lead to resulted the increase in the percentage of Mn^{+3} ion and increase in the percentage of Zn^{+2} ion. Furthermore, EDX analysis revealed that the highest ratio of Zinc atom was 89.05 % at the manganese ratio ion (10wt %).The findings of EDX study demonstrates that the Zn^{+2} and Mn^{+3} ion loads in the final powder is not only fairly similar to one another, but also have excellent compatibility.

Element	series	wt%	At.%
Zn	k-series	73.15	40.01
O	k-series	59.99	26.85
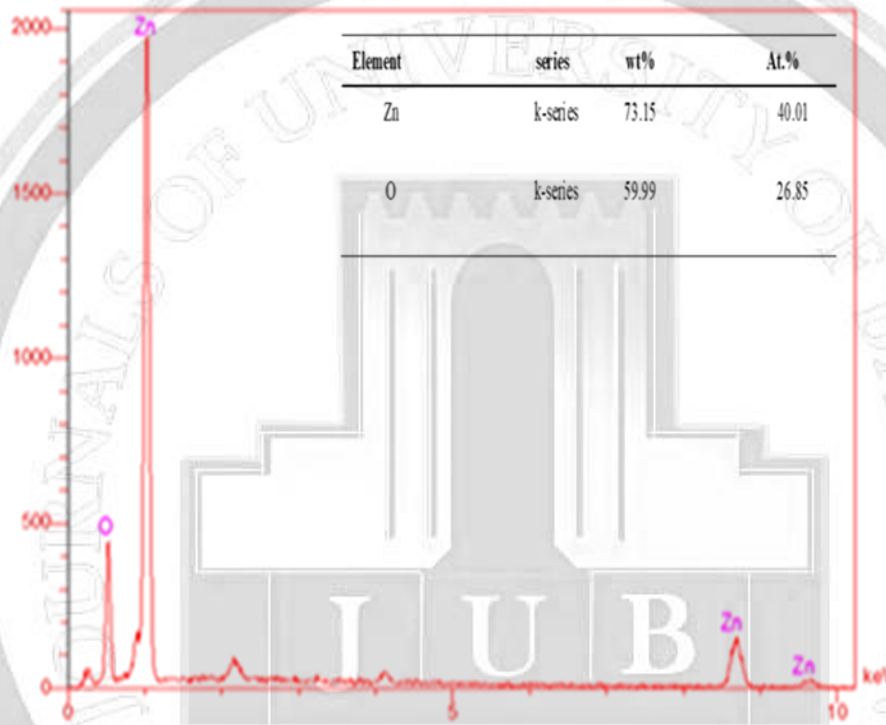
Figure 3. EDX Analysis of Zinc Oxide Nanoparticles ZnO

Element	Series	wt%	At%
Zn	K-series	76.98	47.8
O	K-series	19.14	48.63
Sc	K-series	3.88	3.50
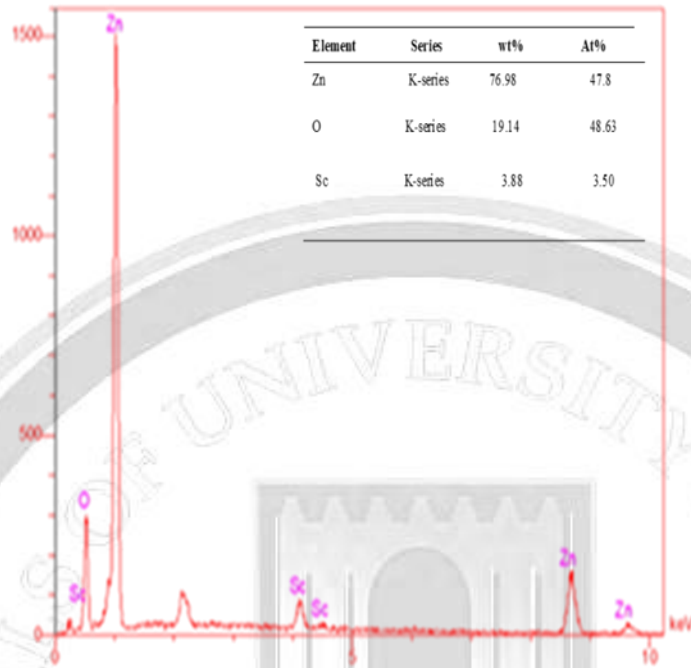
Figure 4. EDX Analys is of Zinc Oxide Nanoparticles Doped with Sc 10 wt% Calcined at 400 °C

Element	series	wt%	At.%
Zn	k-series	89.05	76.18
O	k-series	3.49	12.21
Mn	k-series	6.35	6.46
C	k-series	1.10	5.14
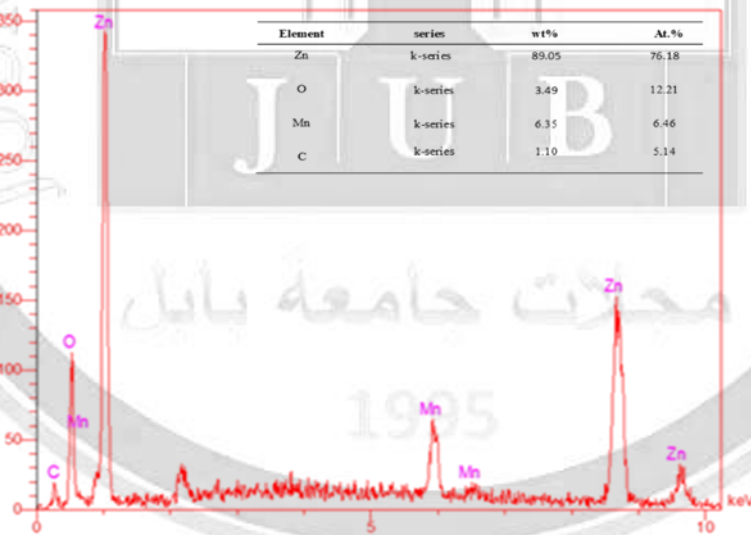
Figure 5 . EDX Analysis of Zinc Oxide Nanoparticles Doped with Mn10 wt%

106

3.3 -Magnetic Properties

In recent years, numerous writers have provided explanations for the room temperature ferromagnetism (RTFM) seen in pure ZnO-NPs, using the room temperature magnetic hysteresis loop (M-H) for ZnO-NPs. [11].Using VSM at the room temperature, magnetization hysteresis loops were performed in order to examine of the magnetic properties of Sc^{+3} ,Mn^{+3} doped ZnO-NPs. For both pure and doped ZnO-NPs, the loops measuring magnetizations against applied magnetic field (M-H) are displayed in Fig6. The present S-like curves, showing room temperature ferromagnetic (RTFM) characteristic. Magnetization due to the tiny crystallite and particle sizes, as well as the tiny amount of magnetic element present in these types of DMS systems were obtained in the pure and doped samples Diluted magnetic semiconductors, transition-metal oxide-doped semiconductors [11-15]. Therefore, it appears that the sample's reported ferromagnetic nature at ambient temperature is inherent. A good reason for the ferromagnetic behavior seen in the room temperature [16,17] (RTFM) in our Sc^{+3},Mn^{+3}. Furthermore, it was practical to believe that the magnetic signal was relative to the vacancies density [18-20]. They were discovered that the pure ZnO nanoparticles displayed, due to the exchange interaction between localized electron spin moments generated from oxygen vacancies in the surface of nanoparticles, they are ferromagnetic at room temperature. The magnetization versus magnetic field [M-H] loops for the $Zn_{1-x}Sc_xO$, $Zn_{1-x}Mn_xO$ (x =0.1wt%). The coercive field at RT is roughly 115.78, 239.4 and 53.32Oe, respectively. The coactivity decreases in (0.1wt%Mn) and increasing (0.1wt%Sc) doping .This difference was caused by the development of a localized magnetic moment, which can happen when the cation flaw is added to the ZnO-NPs host lattice by doping [13]. The value of Ms is 28.34 emu g^{-1} for pure, 37.63 emu $g^{-1}$for 0.1wt%Mn and decrease 9.56 emu g^{-1} for 0.1wt%Sc. As a result, the magnetic moments caused by defects that may have occurred during the synthesis of the ZnO-NPs compound may be the cause of the ferromagnetic behavior seen in these samples. The values of the M against H curve's coercive field (HC) and remanence magnetization (Mr) have a slight magnitudes. As shown in Table 5

Table5. Magnetic Properties of Zinc Oxide Samples

Sample name	HC (Oe)	Ms emu g -1	Mr emu g -1
Pure ZnO	115.78	28.34	2.62
10%Sc	239.4	9.56	2.4
10% Mn	53.32	37.63	1.51
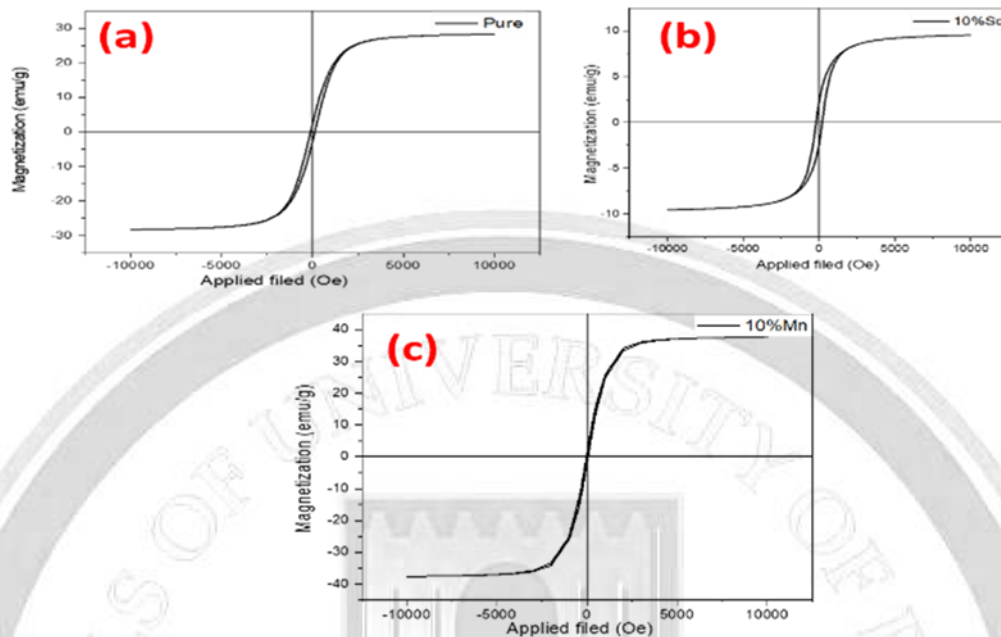
Figure 6 (a) Hysteresis Loops of Pure Zinc Oxide

(b) Hysteresis Loops of Zinc Oxide with 10% Sc

(c) Hysteresis Loops of Zinc Oxide with 10% Mn

2. Conclusion

ZnO doped with the Scandium, manganese was prepared with (10wt%)using co-precipitation method. The characterization XRD research verifies that the ZnO hexagonal wurtzite structure was preserved alongside the (002) preferred crystallized plane for ZnO with (Mn , Sc) added . In FESEM show semispherical shape, and these particles are in the highly agglomerated for ZnO doped Scandium when increase in the manganese amount, higher agglomeration is observed. VSM displays the magnetizations versus applied magnetic field (M-H) loops for the pure and doped ZnO-NPs. The current S-like curves reveal ferromagnetic materials at the room temperature. (RTFM) characteristic.

References

[1] Wolf, S. A., Awschalom, D. D., Buhrman, R. A., Daughton, J. M., von Molnár, V. S., Roukes, M. L., ... & Treger, D. M. (2001). Spintronics: a spin-based electronics vision for the future. *science*, *294*(5546), 1488-1495.

[2] Ghosh, S., Sih, V., Lau, W. H., Awschalom, D. D., Bae, S. Y., Wang, S., ... & Chapline, G. (2005). Room-temperature spin coherence in ZnO. *Applied Physics Letters*, *86*(23).

[3] Dietl, T., Ohno, O. H., Matsukura, A. F., Cibert, J., & Ferrand, E. D. (2000). Zener model description of ferromagnetism in zinc-blende magnetic semiconductors. *science*, *287*(5455), 1019-1022.

[4] Biswal, R. R., Velumani, S., Babu, B. J., Maldonado, A., Tirado-Guerra, S., Castaneda, L., & Olvera, M. D. L. L. (2010). Fluorine doped zinc oxide thin films deposited by chemical spray, starting from zinc pentanedionate and hydrofluoric acid: effect of the aging time of the solution. *Materials Science and Engineering: B*, *174*(1-3), 46-49.

[5] Iribarren, A., Fernández, P., & Piqueras, J. (2008). Cathodoluminescence characterization of ZnO: Te microstructures obtained with ZnTe and TeO2 doping precursors. *Superlattices and Microstructures*, *43*(5-6), 600-604.

[6] Iribarren, A., Fernández, P., & Piqueras, J. (2009). TeO2-doped ZnO micro and nanostructures grown by the vapour–solid technique. *Revista Cubana de Física*, *26*(1), 42-46.

[7] Keskenler, E. F., Doğan, S., Turgut, G., & Gürbulak, B. (2012). Evaluation of structural and optical properties of Mn-doped ZnO thin films synthesized by sol-gel technique. *Metallurgical and Materials Transactions A*, *43*, 5088-5095.

[8] Hardan, R. M., Hameed, A. T., & Radef, W. T. (2023). Biogenic Zirconium Nanoparticles Synthesized from Silybum marianum: A Potent Antibacterial Agent Against Gingivitis bacteria. *Central Asian Journal of Medical and Natural Science*, *4*(5), 1066-1076.

[9] Sharma, P., Gupta, A., Rao, K. V., Owens, F. J., Sharma, R., Ahuja, R., ... & Gehring, G. A. (2003). Ferromagnetism above room temperature in bulk and transparent thin films of Mn-doped ZnO. *Nature materials*, *2*(10), 673-677.

[10] Muktaridha, O., Adlim, M., Suhendrayatna, S., & Ismail, I. (2021). Progress of 3d metal-doped zinc oxide nanoparticles and the photocatalytic properties. *Arabian Journal of Chemistry*, *14*(6), 103175.

[11] Obeid, M. M., Jappor, H. R., Al-Marzoki, K., Al-Hydary, I. A., Edrees, S. J., & Shukur, M. M. (2019). Unraveling the effect of Gd doping on the structural, optical, and magnetic properties of ZnO based diluted magnetic semiconductor nanorods. *RSC advances*, *9*(57), 33207-33221.

[12] Hanish, H. H., Edrees, S. J., & Shukur, M. M. (2020). The effect of transition metals incorporation on the structural and magnetic properties of magnesium oxide nanoparticles. *International Journal of Engineering*, *33*(4), 647-656.

[13] Najem, I. A., Edrees, S. J., & Abd Rasin, F. (2020, November). Structural and Magnetic Characterisations of Pb-Doped MgO Nanoparticles by a Modified Pechini Method. In *IOP Conference Series: Materials Science and Engineering* (Vol. 987, No. 1, p. 012027). IOP Publishing.

[14] Geetha, M. S., Nagabhushana, H., & Shivananjaiah, H. N. (2016). Green mediated synthesis and characterization of ZnO nanoparticles using Euphorbia Jatropa latex as reducing agent. *Journal of Science: Advanced Materials and Devices*, *1*(3), 301-310.

[15] Yumak, A., Turgut, G., Kamoun, O., Ozisik, H., Deligoz, E., Petkova, P., ... & Goumri-Said, S. (2015). Stability and morphology-dependence of Sc3+ ions incorporation and substitution kinetics within ZnO host lattice. *Materials Science in Semiconductor Processing*, *39*, 103-111.

[16] Karmakar, R., Neogi, S. K., Banerjee, A., & Bandyopadhyay, S. (2012). Structural; morphological; optical and magnetic properties of Mn doped ferromagnetic ZnO thin film. *Applied surface science*, *263*, 671-677.

[17] Pazhanivelu, V., Selvadurai, A. P. B., Kannan, R., & Murugaraj, R. (2016). Room temperature ferromagnetism in Ist group elements codoped ZnO: Fe nanoparticles by co-precipitation method. *Physica B: Condensed Matter*, *487*, 102-108.

[18] Coey, J. M. D., Venkatesan, M., & Fitzgerald, C. B. Nature Mater. 4, 173–179 (2005). *CrossRef| PubMed| CAS| Web of Science® Times Cited*, *616*.

[19] Kumar, A., Kumar, J., & Priya, S. (2012). Defect and adsorbate induced ferromagnetic spin-order in magnesium oxide nanocrystallites. *Applied Physics Letters*, *100*(19).

[20] Freund, M. M., Freund, F., & Batllo, F. (1989). Highly mobile oxygen holes in magnesium oxide. *Physical review letters*, *63*(19), 2096.

تحضير وتوصيف جزيئات $Zn_{0.9}Sc_{0.1}O,Zn_{0.9}Mn_{0.1}O$ ومقارنتها مع NPs من أكسيد الزنك بأستخدام طريقه الترسيب

مريم غسان غفار   **شاكر جاهل ادريس**

جامعه بابل /كليه هندسه المواد قسم السيراميك ومواد البناء

mariam35@ghassangmail.com

الخلاصه

تم تحضير ماده نقيه من ZnO وتم اضافه السكانديوم(Sc^{+3}) والمنغنيز (Mn^{+3}) بنسب مختلفه بصيغه $Zn_{(1-x)}Sc_xO,Zn_{(1-x)}Mn_xO$ ثم تصنيعها بطريقه الترسيب . وبشكل خاص فقد ثبتت أن العديد من خصائص الفيزيائيه الجديده والمثيره للاهتمام تم أنشاؤها عن طريق مزيج من البحوث المرفولوجيه والبنيويه والبصريه. أوضحت الأبحاث أن حيود الاشعه السينيه أنه تم الحفاظ على بنيه wurtzite السداسيه من أكسيد الزنك الى جانب المستوى المتبلور(002) وكذلك عن أضافه ايونات (Mn,Sc) مع أكسيد الزنك. عند فحص العينات باستخدام المجهر الالكتروني ظهر الشكل النصف كروي وكلما زادت كميه المنغنيزكلما لوحظ وجود تكتل اعلى . وتمت الاشاره الى أن فحص المغناطيسيه تم استخدامه للحصول على حلقات الهستره . تظهر ZnO-NPs خاصيه مغناطيسيه في درجه حراره الغرفه.

الكلمات الدالة : أشبه الموصلات المغناطيسيه المخففه, أكسيد الزنك , المنغنيز , سكانديوم , XRD,FESEM,VSM